Am J Cancer Res 2025;15(12):5301-5316
www.ajcr.us /ISSN:2156-6976/ajcr0167424

Original Article

DERL3 exacerbates glioblastoma malignancy through endoplasmic reticulum stress-dependent mechanisms

Shaoqi Du[1*], Shuo Zhang[2*], Chen Li[3*], Shaonan Du[4], Shu Guan[5], Shiyang Wang[6], Zhe Wang[6], Tao Dong[6], Xiaolin Ren[6]

[1]Department of Operating Room, China-Japan Union Hospital of Jilin University, Changchun 130033, Jilin, China; [2]Department of Operating Room, Shengjing Hospital of China Medical University, Sanhao Street 36, Heping District, Shenyang 110004, Liaoning, China; [3]Department of Orthodontics, The First Clinic of Stomatological Hospital of China Medical University, Shenyang 110063, Liaoning, China; [4]Department of Neurosurgery, Shengjing Hospital of China Medical University, Sanhao Street 36, Heping District, Shenyang 110004, Liaoning, China; [5]Department of Surgical Oncology and Breast Surgery, First Hospital of China Medical University, Nanjing Street 155, Heping District, Shenyang 110001, Liaoning, China; [6]Department of Neurosurgery, Shenyang Red Cross Hospital, No. 389 Zhongshan Road, Shenhe District, Shenyang 110013, Liaoning, China. [*]Equal contributors.

Received July 13, 2025; Accepted December 14, 2025; Epub December 25, 2025; Published December 30, 2025

Abstract: Gliomas, particularly glioblastoma multiforme (GBM), represent the most prevalent primary intracranial malignancies, characterized by high invasiveness, aggressive proliferation, and poor clinical outcomes. Recent studies have highlighted the critical role of tumor microenvironment interactions and cellular stress responses, including endoplasmic reticulum (ER) stress, in modulating glioma progression. While ER stress can induce autophagy and apoptosis, glioma cells exhibit remarkable plasticity, adapting to stress conditions and exploiting them to promote survival and self-renewal, thereby contributing to therapeutic resistance. In this study, we established an individualized ER stress risk score using glioma transcriptomic data, demonstrating its association with adverse prognosis, aggressive molecular subtypes, and pro-tumorigenic biological functions. Through systematic screening, we identified DERL3 as a core effector gene mediating ER stress adaptation. Functional validation revealed that DERL3 drove glioma proliferation and invasion by binding to and stabilizing Heterogeneous nuclear ribonucleoprotein A2/B1 (HNRNPA2B1), consequently activating the NF-κB signaling pathway. These findings elucidate the DERL3-HNRNPA2B1-NF-κB axis as a critical mechanistic link between ER stress adaptation and glioma malignancy. Targeting this axis may offer novel therapeutic strategies to overcome treatment resistance, providing significant translational potential for improving glioma management. This study advances our understanding of stress response mechanisms in tumorigenesis and underscores the clinical relevance of ER stress-related pathways in precision oncology.

Keywords: Endoplasmic reticulum stress, glioblastoma, tumorigenesis, DERL3, heterogeneous nuclear ribonucleoprotein A2/B1 (HNRNPA2B1)

Introduction

Glioma represents the most prevalent primary brain tumor and is associated with the highest rates of intracranial disability and mortality among central nervous system (CNS) malignancies [1, 2]. Glioblastoma multiforme (GBM), the most aggressive glioma subtype, exhibits a median survival of merely 14.6 months despite intensive multimodal therapy, including surgical resection, radiotherapy and chemotherapy [3, 4]. This dismal prognosis is a direct consequence of GBM's hallmark features: extensive invasiveness, relentless proliferation, and remarkable microenvironmental adaptability. Recent studies have demonstrated that various extrinsic signals or therapeutic interventions frequently induce a high-stress state in tumor cells [5]. While such stress conditions can trigger tumor cell autophagy and apoptosis, thereby exerting antitumor effects, glioma cells like many other malignancies rapidly develop therapeutic resistance [6]. This adaptive response primarily results from their intrinsic plasticity

and capacity to transform stress signals into drivers of self-renewal. Therefore, elucidating the key signaling targets and mechanisms that govern this adaptive response is of paramount importance for understanding glioma pathogenesis and developing novel therapeutic strategies.

Accumulating evidence implicates endoplasmic reticulum (ER) stress activation in the pathogenesis and progression of malignant tumors [7, 8]. Multiple factors can induce ER stress, including radiotherapy, chemotherapy, oxidative stress, nutrient deprivation, and inflammatory responses [9]. Upon ER stress activation, tumor cells rapidly initiate adaptive protective mechanisms, notably the unfolded protein response (UPR). Emerging research indicates that UPR can activate the HIF1α signaling pathway, a well-established mediator of tumor cell proliferation, invasion, migration, angiogenesis, and glycolytic metabolism. In triple-negative breast cancer, IRE1α facilitates formation of XBP1-HIF1α transcriptional complexes that recruit RNA polymerase II to regulate HIF1α target genes, thereby promoting cancer cell proliferation and invasion [10]. Jiang et al. further demonstrated that IRE1α activation induces IκB phosphorylation and degradation through interaction with tumor necrosis factor receptor eLF2α, subsequently activating NF-κB signaling [11].

Current therapeutic strategies increasingly target ER stress or modulate associated pathways to influence tumor progression. For instance, ER stress-induced exosomal miR-27a-3p promotes breast cancer immune escape by regulating PD-L1 expression in macrophages [12]. The ER stress mediator ERO1 triggers cancer metastasis by activating angiogenesis under hypoxia [13]. In lung adenocarcinoma, p62 induces autophagy-mediated upregulation of NRF2 and ATF6, driving tumor progression [14]. However, the mechanisms through which ER stress influences glioma pathogenesis remain poorly understood. Systematic analysis of ER stress status in gliomas and identification of relevant molecular markers therefore carry substantial scientific and clinical significance.

While the derlin family protein DERL3, a key component of the ER-associated degradation (ERAD) machinery, has been implicated in the progression of cancers such as lung adenocarcinoma and breast cancer [15, 16], its specific role, regulatory mechanisms, and clinical significance in glioblastoma have remained largely unexplored. Our work is the first to identify DERL3 as a core effector within the ER stress network in GBM, to delineate its specific regulation by the ATF6 branch of the UPR, and to uncover the novel DERL3-HNRNPA2B1-NF-κB axis as a critical link between ER stress adaptation and glioma malignancy.

In this study, we systematically analyzed ER stress-related signatures in glioma, establishing a robust association between ER stress activation and aggressive molecular subtypes and poor patient prognosis. Through functional genomics and experimental validation, we pinpointed DERL3 as a central mediator of ER stress-driven oncogenicity. We further demonstrate that DERL3 exerts its pro-tumorigenic effects by binding to and stabilizing the RNA-binding protein HNRNPA2B1, leading to the consequential activation of the NF-κB pathway. These findings not only position DERL3 as a promising prognostic biomarker and therapeutic target but also provide a novel mechanistic framework for how ER stress fuels GBM aggressiveness.

Materials and methods

Ethics statement

The experimental protocol received approval from the Ethics Committee of Shenyang Red Cross Hospital. All animal studies were performed in compliance with the guidelines set forth by the Shenyang Red Cross Hospital Animal Care and Use Committee and were further approved by the Institutional Review Board of Shenyang Red Cross Hospital.

Clinical specimens

For Western blot analysis, 26 surgically resected glioma specimens (4 non-tumor controls, 8 WHO grade II, 7 grade III, and 7 grade V) were obtained between January 2018 and October 2020. Immunohistochemical (IHC) studies utilized 61 specimens (6 non-tumor, 10 grade II, 24 grade III, and 31 grade IV) collected from February 2014 to October 2020.

Cell culture models

Human glioma cell lines (U87, U251, LN229) were obtained from the Chinese Academy of Sciences Cell Bank (Shanghai, China). Normal human astrocytes (NHA) were kindly provided

by Prof. Jiang Tao (Beijing Neurosurgical Institute). Primary glioblastoma stem-like cells (GSC21, GSC40) were established in our laboratory from fresh surgical specimens under approved protocols.

RNA isolation and qRT-PCR

Total RNA was extracted using TRIzol reagent (Takara) following manufacturer's protocol. RNA purity and concentration were determined spectrophotometrically (NanoDrop). cDNA synthesis was performed using PrimeScript RT Master Mix (Takara). Quantitative PCR utilized SYBR Green Master Mix (Takara) on a QuantStudio system with cycling conditions: 95°C for 30 s, followed by 40 cycles of 95°C for 5 sec and 60°C for 30 sec. Relative mRNA expression was calculated via the $2^{-\Delta\Delta Ct}$ method using 18S rRNA as endogenous control.

Protein blotting

Protein lysates were quantified by BCA assay. For immunoblotting, 20 μg protein/lane was separated by 10% SDS-PAGE and transferred to PVDF membranes. After blocking with 5% non-fat milk, membranes were incubated with primary antibodies (4°C overnight) followed by HRP-conjugated secondary antibodies (1 h, RT). Signals were developed using ECL substrate and quantified by ImageJ.

Immunohistochemistry (IHC)

Formalin-fixed paraffin sections underwent antigen retrieval in citrate buffer (pH 6.0), endogenous peroxidase blocking (3% H_2O_2), and serum blocking. Primary antibodies were applied overnight at 4°C. Detection used biotin-streptavidin-HRP system with DAB chromogen. Sections were counterstained with hematoxylin, dehydrated, and mounted.

Endoplasmic reticulum stress activation and inhibition experiments

The U87 and LN229 cells were seeded at a density of 500,000 cells per well in a six-well plate. When the cell density reached 70%, the experimental group was treated with 1 μM endoplasmic reticulum stress activator Thapsigargin (tartrazine), while the control group received PBS. After 48 hours, the expression of target proteins was detected. The experimental group was also treated with 2 mM endoplasmic reticulum stress inhibitor Tauroursodeoxycholate Sodium (sodium taurocholate), and the control group received PBS. After 48 hours, the expression of target proteins was detected again.

Cell proliferation assay

After 60 hours of cell transfection, the cells were seeded at a density of 1000 per well into a 96-well plate, with a total volume of 100 μl per well. The plates were cultured for 5 days under conditions of 37°C and 5% CO_2. At the same time on days 0, 1, 2, 3, 4, and 5, 20 ul MTS solution (Promega) was added to each well and incubated at 37°C for 3 hours. The optical density (OD) values of each well were measured using an Molecular Devices (Spectramax M5) spectrophotometer at 490 nm to assess the proliferation capability of the cells.

Detection of cell invasion, migration and cell cloning ability

The invasive and migratory abilities of cells were detected using a 24-well plate and Transwell chambers. Cells ($5*10^4$ for the migration test; $1*10^5$ for the invasion test) were seeded in the upper chamber with a medium containing 0.2% FBS (the invasion chamber was coated with 80 μl of a 1:8 diluted matrix gel). The lower chamber was filled with a medium containing 20% fetal bovine serum. After culturing for 16 h and 24 h, respectively, the cells were washed with PBS, fixed with 4% paraformaldehyde, and stained with 0.1% crystal violet. Under 100× magnification, the number of cells was counted in five random areas. In the cell clonal experiment, 2000 cells were seeded in a 6-well plate. Two weeks later, the cells were fixed with methanol and then stained with 0.1% crystal violet, and the number of visible colonies was counted. In the overexpression group, the invasive and migratory abilities were enhanced.

Immuno-coimmunoprecipitation (Co-IP) experiment

Take $1*10^7$ cells and use the IP-specific lysis buffer as instructed to lyse the cells. Then, after lysis on a 4°C rotor for 3 hours, centrifuge to collect the supernatant. Add A/G magnetic beads to the rotor and incubate for 10 minutes before collecting the supernatant again to prevent non-specific protein binding. In a new EP

tube, take 30 μl of protein as the Input group for this experiment, then add 300 μl of protein along with the corresponding IP antibodies as the IP group. Another tube should be added with IgG antibodies as the control. The above antigen-antibody complexes are incubated overnight in a 4-degree rotor. The next day, add magnetic beads to the antigen-antibody complexes, mix at room temperature, and incubate on a rotor for 120 minutes. Collect the antigen-antibody complexes using a magnetic force frame, add 1× loading buffer of heat, denature the protein, and proceed with Western Blot detection.

Protein stability test

After 48 h of cell transfection, wash with PBS; to investigate the protein degradation rate under different treatment conditions, add 20 mM Cycloheximide (CHX) to each group to inhibit protein synthesis in cells, and detect the expression of target proteins at 0 h, 3 h, 6 h, and 9 h. To further explore the protein degradation pathway, add 20 uM proteasome inhibitor MG132 or 20 uM lysosome inhibitor Chloroquine (CQ) simultaneously with CHX, and detect the expression of target proteins at 0 h, 3 h, 6 h, and 9 h.

Animal studies

Male BALB/c nude mice aged 4 to 6 weeks were purchased from Beijing Vital River Laboratory Animal Technology. All mice were housed under specific pathogen-free (SPF) conditions. The mice were maintained on a 12-hour light/dark cycle, with the temperature and humidity of the rearing environment set at 18-22°C and 50-60%, respectively. When humane endpoints were reached (neurological deficits, ≥20% weight loss, or marked lethargy), mice were sacrificed by intraperitoneal injection of sodium pentobarbital (150 mg/kg). This overdose rapidly induced deep anesthesia, unconsciousness, and respiratory arrest; death was confirmed by loss of corneal/pedal reflexes and cessation of heartbeat.

Intra-cerebral transplantation of nude rats

Using a stereotactic instrument, $5*10^5$ U87 cells with different treatment factors were injected into the substantia nigra of the right brain of nude mice, with a vertical depth of 3 mm. When neurofunctional symptoms appeared in tumor-bearing mice, euthanasia was performed simultaneously on different groups of mice, and the brain tissue was fixed and embedded, followed by HE staining and immunohistochemical staining; the above experiment was repeated to investigate survival differences under different conditions.

Bioinformatics analysis

The clinical expression profiles and molecular data required for the study were obtained from three publicly available and shareable data sources: the American Cancer Genome Atlas (The Cancer Genome Atlas, TCGA), the International Neuroglial Gene Atlas Database (Chinese Glioma Genome Atlas, CGGA), GlioVis glioma data platform. The gene sets related to endoplasmic reticulum stress were selected from the GSEA website-(http://www.gseamsigdb.org/gsea/ msigdb/search.jsp), activated endoplasmic reticulum stress genes set [18]: GO_REF: 0000058; inhibited endoplasmic reticulum stress genes set [19]: GO_REF: 0000058. Using the CGGA RNA-seq, TCGA RNA-seq, CGGA microarray glioma expression profile and clinical data, univariate COX regression was applied to identify endoplasmic reticulum stress-related genes with prognostic significance. The ssGSEA algorithm was used to weight and screen out the relevant gene expression levels and clinical prognosis data from the database, calculating the endoplasmic reticulum risk score for each sample. The CGGA database's clinical prognosis and molecular subtype data were utilized to demonstrate the correlation between endoplasmic reticulum risk scores and various molecular subtypes, grades, and prognoses.

Statistical analysis

Using GraphPad Prism 8 (GraphPad Software Inc, La Jolla, CA) and R language (version 3.6.1; R packages: pheatmap, corrplot) for statistical data analysis and plotting. A one-way COX regression was performed using R; the ROC curve was plotted using Medcalc19.0.7 (www.medcalc.org); survival analysis was conducted using the Kaplan-Meier method with log-rank tests; KEGG enrichment analysis was used to identify relevant signaling pathways. The results are presented as means ± standard error of mean (SEM). For multiple-group comparisons, one-way analysis of variance (ANOVA)

was applied, followed by appropriate post-hoc tests based on experimental design: Tukey's honest significant difference (HSD) test for pairwise comparisons among all groups, Bonferroni's test for planned comparisons, or Dunnett's test for comparisons against a control group. * means $P<0.05$, ** means $P<0.01$, *** means $P<0.001$, **** means $P<0.0001$.

Results

DERL3 as a core ER stress-related gene associated with poor prognosis in GBM

To identify prognostic ER stress-related genes, we analyzed 81 genes from the GESA database using univariate COX regression in the CGGA dataset. Seven genes showed significant survival associations (P<0.0001), with *PPP1R15A*, *FCGR2B*, *EDEM1*, *DERL3*, and *OS9* as risk factors (HR>1), and *UBXN1* and *UBQLN1* as protective (HR<1). An ER stress risk score derived from these genes correlated with aggressive glioma subtypes (e.g., mesenchymal, IDH-wildtype) and higher WHO grades (**Figures 1A** and S1A). High-risk patients had worse survival (**Figure 1B**). Multivariate analysis identified *DERL3* as an independent prognostic marker, validated by ROC curves in CGGA and TCGA datasets (Figure S1B-F). Elevated *DERL3* expression predicted poorer survival across grades, especially in GBM (Figure S2A-F), and stratified outcomes by MGMT and IDH status (Figure S2G-L). *DERL3* increased with tumor grade (Figure S3A-C) and was highest in mesenchymal GBM and IDH-wildtype tumors (Figure S3D-I). Histopathological validation via immunohistochemistry corroborated these findings, demonstrating a progressive upregulation of DERL3 with increasing tumor grade (**Figure 1C**). Additional mRNA and protein-level analyses in glioma tissues further confirmed that DERL3 expression escalates with advancing malignancy (**Figure 1D-F**).

DERL3 promotes malignant progression of GBM cells

To assess the expression profile of DERL3 in glioma cells, we analyzed its mRNA and protein levels in human glioma cell lines (U87, U251, LN229), primary glioma stem-like cells (GSC21, GSC40), and normal human astrocytes (NHA). Notably, DERL3 expression was significantly elevated in glioma cell lines compared to NHA, with particularly high levels observed in LN229 and U87 cells (**Figure 2A**). To investigate the functional role of DERL3 in glioma progression, we established stable DERL3-knockdown models in U87 and LN229 cells using lentiviral shRNA constructs. Quantitative PCR and Western blotting confirmed efficient DERL3 silencing at both transcriptional and translational levels (**Figure 2B**).

Functional assays revealed that *DERL3* knockdown markedly suppressed glioma cell proliferation. MTS assays demonstrated a significant reduction in cell viability over time in DERL3-depleted U87 and LN229 cells compared to controls (**Figure 2C**). Consistent with this, colony formation assays indicated impaired clonogenic capacity upon DERL3 suppression (**Figure 2D**). To evaluate the impact of DERL3 on glioma cell motility, we performed Transwell migration and Matrigel invasion assays. *DERL3* knockdown resulted in a substantial decrease in both migratory and invasive capacities, as evidenced by reduced cell penetration through the membrane pores and Matrigel matrix (**Figure 2E**, **2F**). To further validate these findings, we generated *DERL3*-overexpressing U87 and LN229 cells via plasmid transfection (Figure S4A, S4B). Functional assays demonstrated that *DERL3* overexpression significantly enhanced glioma cell migration and invasion compared to vector controls (Figure S4C, S4D). Collectively, these data indicate that DERL3 plays a critical role in promoting glioma cell proliferation, migration, and invasion, underscoring its potential as a key driver of GBM malignancy.

ATF6-mediated DERL3 regulation drives GBM malignancy through ER stress activation

Our initial findings established DERL3 as an ER stress-responsive gene contributing to glioma malignancy. To investigate the regulatory mechanism, we pharmacologically modulated ER stress in U87 and LN229 cells. Treatment with thapsigargin, an ER stress inducer, significantly upregulated both classical ER stress markers (ATF6 and BiP) and DERL3 expression (**Figure 3A**). Conversely, the ER stress inhibitor tauroursodeoxycholate sodium (TUDCA) suppressed ATF6, BiP and DERL3 levels (**Figure 3A**). To identify the specific ER stress pathway govern-

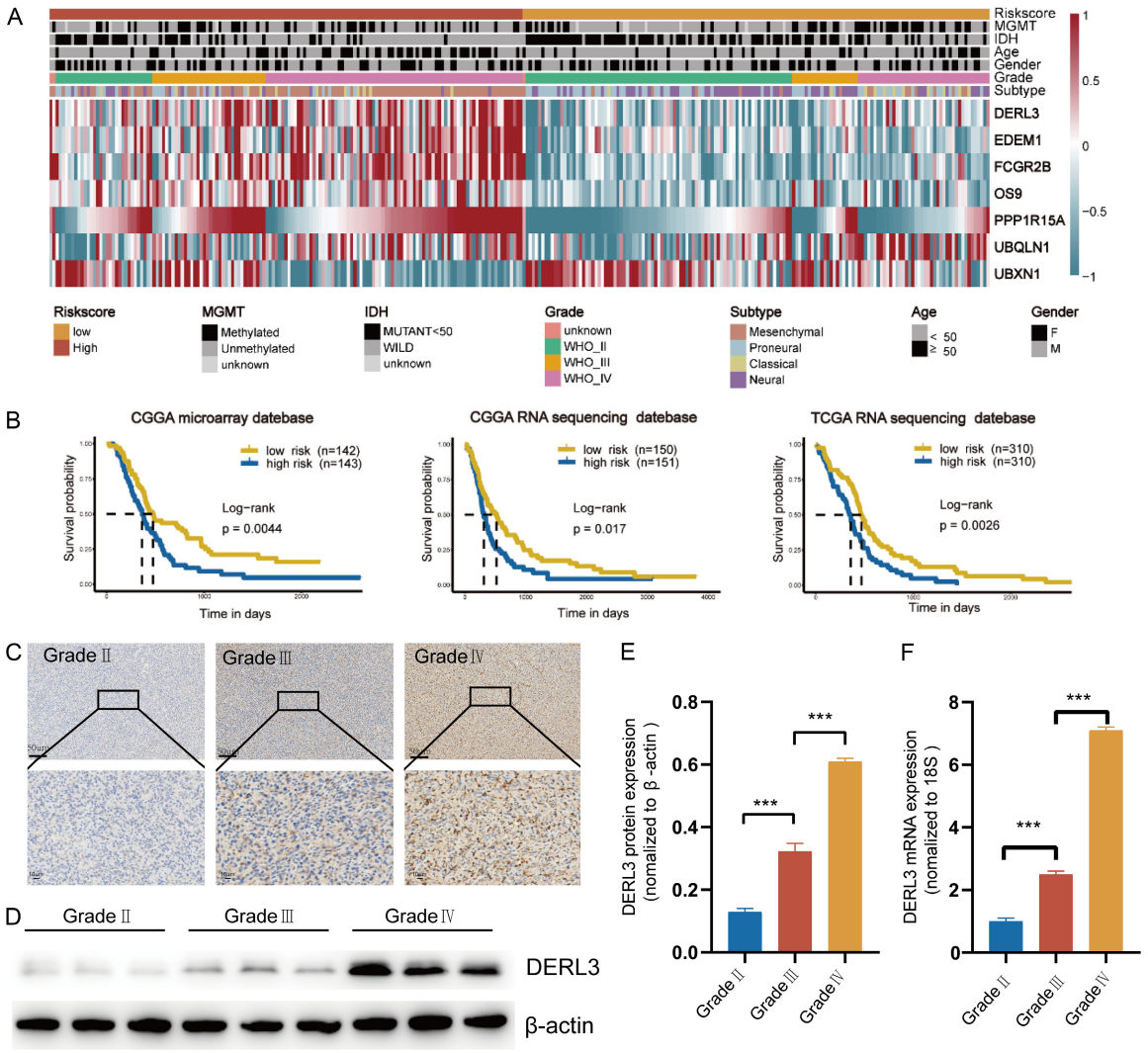

Figure 1. Endoplasmic reticulum stress, mediated by DERL3, drives malignant progression in glioma. A. Expression patterns and clinical relevance of the seven constitutive risk score genes in the CGGA database. B. Survival analysis comparing high- vs. low-ERS risk groups in the three databases. C. Immunohistochemical staining of DERL3 in glioma tissues (grades II-IV) (DERL3 antibody for IHC, abcam: ab78233; magnification: Upper for 10X and Lower for 20X). D, E. Protein levels of DERL3 across glioma grades (II-IV) (DERL3 antibody for WB, Santa cruz: sc-390289; β-actin antibody, CST: 3700) (n=3, one-way ANOVA). F. mRNA expression of DERL3 in glioma grades II-IV (n=3, one-way ANOVA).

ing DERL3 expression, we performed comprehensive correlation analysis in the CGGA glioma dataset. Among the three major ER stress branches (PERK-eIF2α-ATF4, ATF6, and IRE1-XBP1 pathways), DERL3 showed the strongest positive correlation with ATF6 (Figure S4E). Subsequent experimental validation confirmed this regulatory relationship: *ATF6* knockdown markedly decreased DERL3 protein levels (**Figure 3B**), while *DERL3* silencing had no reciprocal effect on ATF6 expression (**Figure 3C**), demonstrating unidirectional regulation of DERL3 by ATF6.

Functional characterization revealed that ER stress activation significantly enhanced the proliferative, migratory and invasive capacities of glioma cells (**Figure 3D-F**). Importantly, this pro-tumorigenic effect was substantially attenuated in *DERL3*-knockdown cells (**Figure 3D-F**), indicating that DERL3 mediates the malignancy-promoting effects of ER stress in glioma. These findings establish the ATF6-DERL3 axis as a critical mechanistic link between ER stress and GBM progression, suggesting that targeting this pathway may represent a novel therapeutic strategy for GBM treatment.

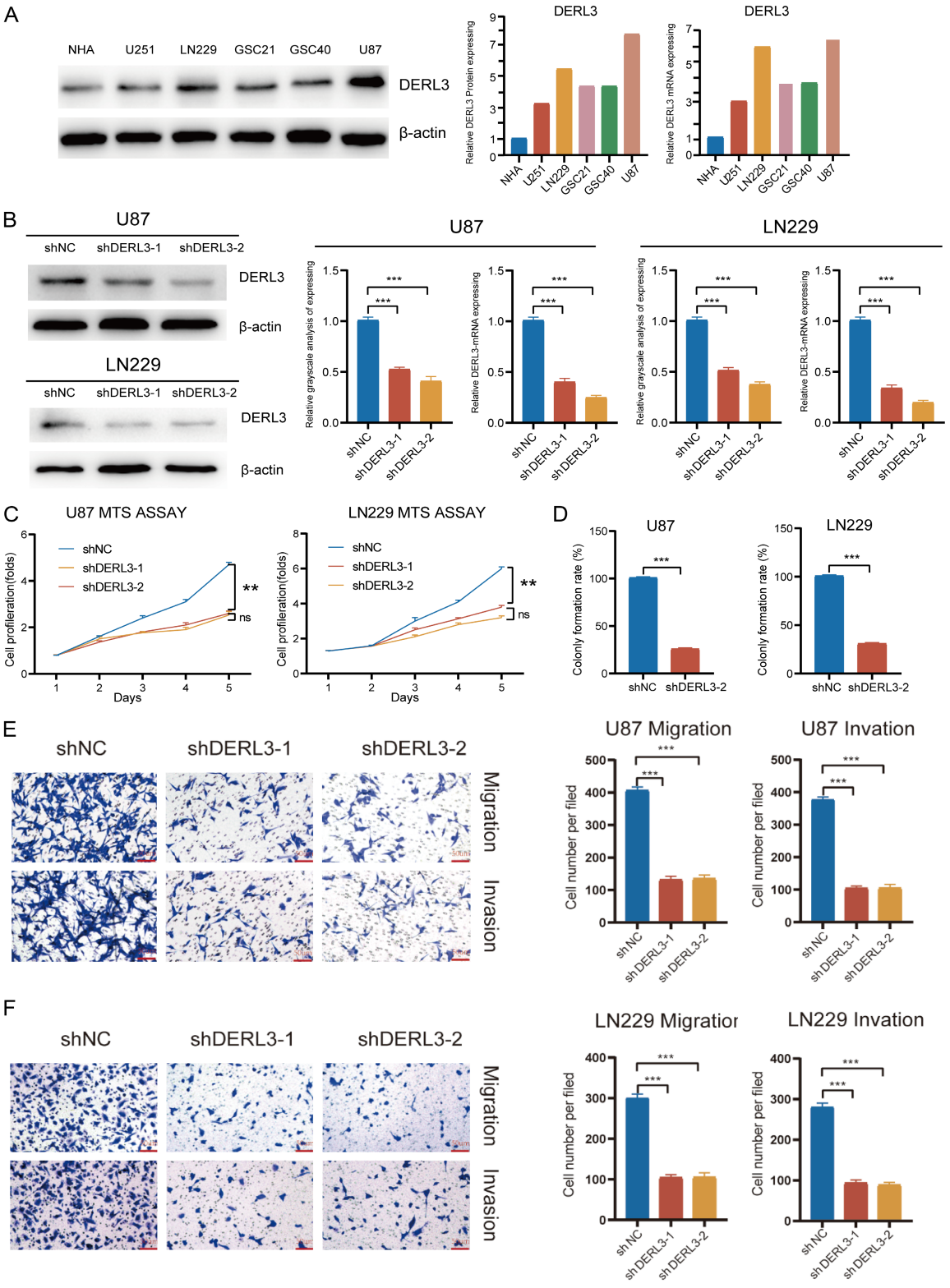

Figure 2. Knockdown of DERL3 suppresses malignant phenotypes in GBM. A. Protein expression and mRNA expression of DERL3 across different cell lines. B. Validation of DERL3 knockdown efficiency in U87 and LN229 cells (n=3, one-way ANOVA). C. Proliferation curves of U87 and LN229 cells after DERL3 knockdown (n=3, two-way repeated-measures ANOVA). D. Colony formation ability of U87 and LN229 cells upon DERL3 knockdown (n=3, one-way ANOVA). E, F. Effects of DERL3 knockdown on invasion and migration in U87 and LN229 cells (n=3, one-way ANOVA; Magnification: 10X).

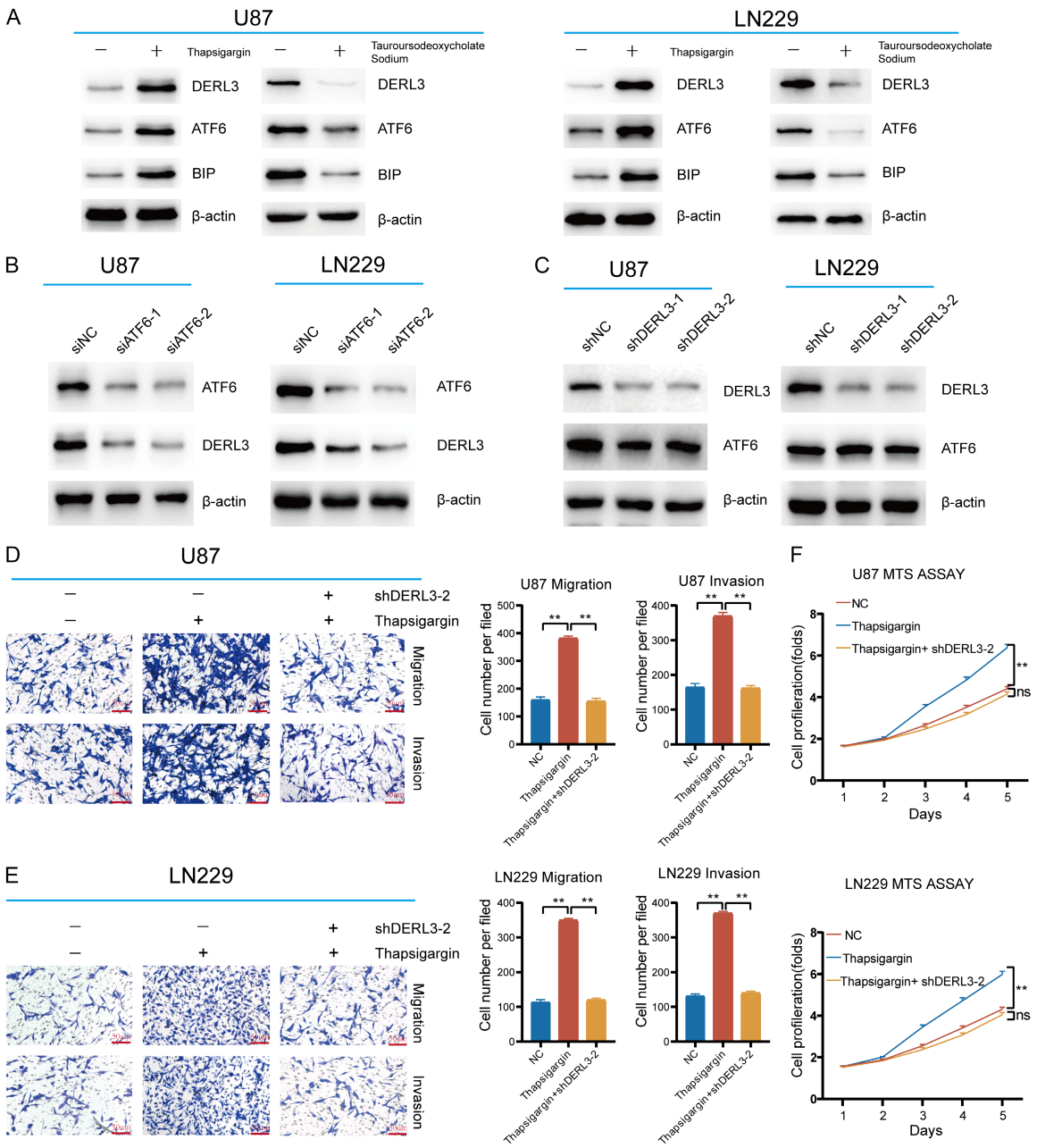

Figure 3. Protein expression and malignant behavior detection of various molecules in GBM cells under endoplasmic reticulum stress and inhibition states. A. The protein expression of various related genes in U87 and LN229 cells under different treatment factors of endoplasmic reticulum stress activators and inhibitors (ATF6 antibody, CST: 65880; BIP antibody, CST: C50B12). B. ATF6 could regulate DERL3 expression in U87 and LN229 cells. C. ATF6 could not be regulated by DERL3 in U87 and LN229 cells. D, E. Detection of cell migration and invasion after knocking down DERL3 and administering endoplasmic reticulum stress activator (n=3, one-way ANOVA; Magnification: 10X). F. Detection of cell proliferation ability after knocking down DERL3 and administering endoplasmic reticulum stress activator (n=3, two-way repeated-measures ANOVA).

DERL3 promotes GBM malignancy by activating the NF-κB signaling pathway

KEGG pathway enrichment analysis revealed significant enrichment of differentially expressed genes between *DERL3*-high and *DERL3*-low expression groups in the NF-κB signaling pathway (**Figure 4A**). Subsequent western blot validation demonstrated that *DERL3* knockdown resulted in marked downregulation of phosphorylated NF-κB protein levels, while total NF-κB expression remained unaltered (**Figure**

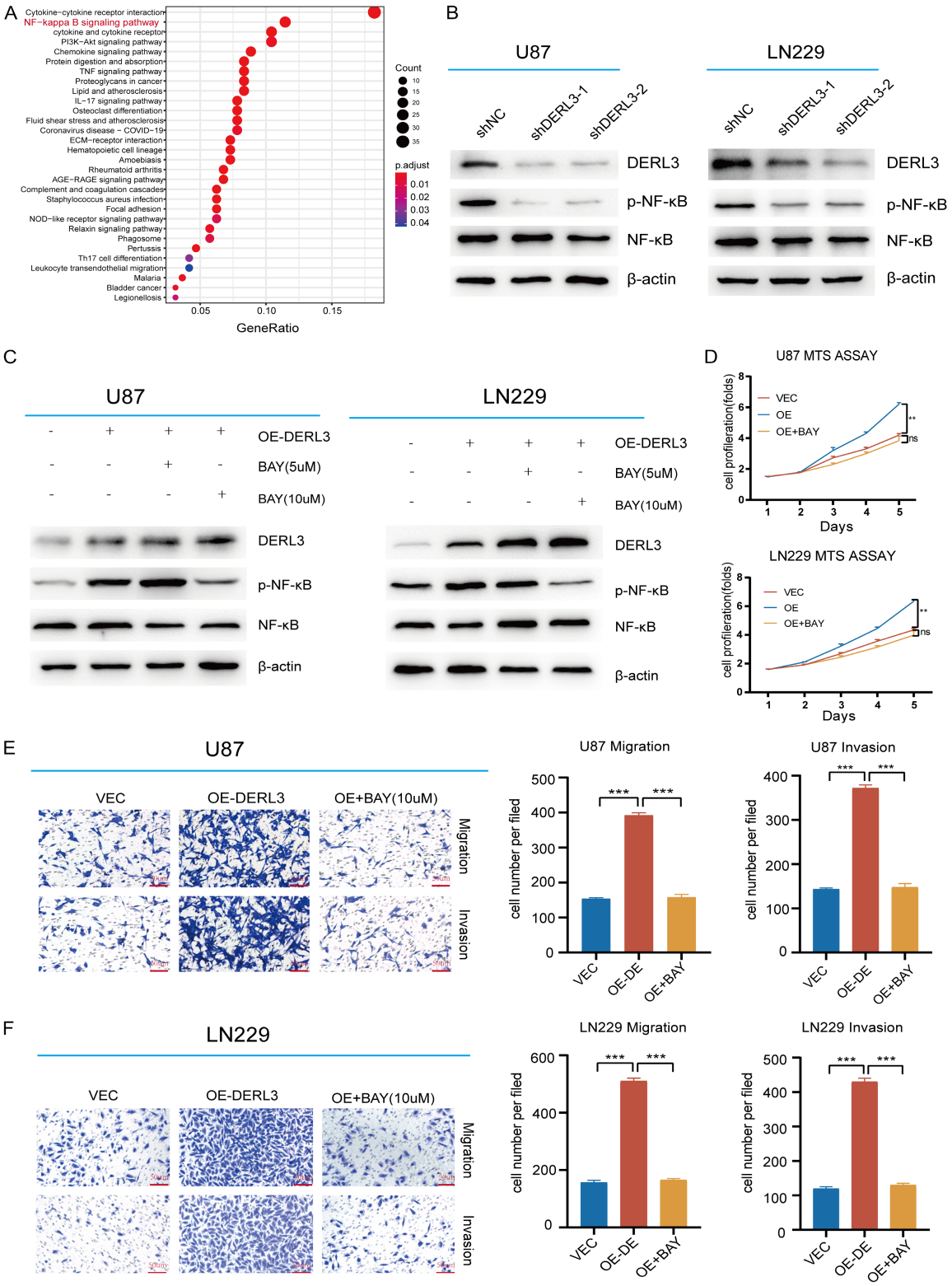

Figure 4. DERL3 promotes GBM cell invasion via NF-κB signaling pathway regulation. A. KEGG pathway analysis of differentially expressed genes associated with DERL3 in the CGGA GBM database. B. Western blot analysis of NF-κB pathway activity following DERL3 knockdown in LN229 and U87 cells (NF-κB antibody, CST: 8242; p-NF-κB antibody, CST: 3033). C. Western blot validation of NF-κB activation upon DERL3 overexpression and treatment with varying BAY (NF-κB inhibitor) concentrations in U87 and LN229 cells. D. Impact of DERL3 overexpression ± BAY on glioma cell proliferation (n=3, two-way repeated-measures ANOVA). E, F. Effects of DERL3 overexpression ± BAY on glioma cell migration and invasion (n=3, one-way ANOVA; Magnification: 10X).

4B). To further elucidate the functional involvement of DERL3 in glioma progression via NF-κB signaling, we performed pharmacological inhibition experiments using the specific NF-κB inhibitor BAY 11-7082. Dose-response analysis in DERL3-overexpressing cells showed that 10 μM BAY 11-7082 effectively suppressed NF-κB protein expression (**Figure 4C**). Notably, this treatment abrogated the pro-malignant effects mediated by DERL3 overexpression, as evidenced by significant attenuation of glioma cell aggressiveness (**Figure 4D-F**). These findings collectively demonstrate that DERL3 promotes glioma malignancy through activation of the NF-κB signaling pathway.

DERL3 interacts with HNRNPA2B1 and regulates its protein stability

To further elucidate the molecular mechanisms underlying DERL3-mediated promotion of glioma malignancy, we sought to identify potential binding partners of DERL3. Immunoprecipitation (IP) coupled with mass spectrometry analysis revealed HNRNPA2B1 as a putative interacting protein of DERL3, a finding subsequently validated by co-immunoprecipitation (Co-IP) assays (**Figure 5A**). Intriguingly, knockdown of DERL3 led to a marked reduction in HNRNPA2B1 protein levels (**Figure 5B**), whereas its mRNA expression remained unchanged (**Figure 5C**), suggesting post-transcriptional regulation of HNRNPA2B1 by DERL3.

To determine whether DERL3 stabilizes HNRNPA2B1 through direct binding, we performed cycloheximide (CHX) chase assays to assess HNRNPA2B1 protein turnover. Notably, DERL3 depletion significantly accelerated HNRNPA2B1 degradation (**Figure 5D**), supporting a role for DERL3 in maintaining HNRNPA2B1 stability. Further investigation into the degradation mechanism revealed that the proteasome inhibitor MG132, but not the lysosome inhibitor chloroquine (CQ), attenuated HNRNPA2B1 degradation (**Figure 5E**, **5F**), indicating that HNRNPA2B1 turnover is primarily mediated by the ubiquitin-proteasome pathway.

DERL3 activates NF-κB signaling through HNRNPA2B1-dependent mechanisms

To investigate the functional relationship between DERL3 and HNRNPA2B1 in NF-κB pathway activation, we first established stable *HNRNPA2B1*-knockdown models in LN229 and U87 glioma cell lines. Western blot analysis demonstrated that HNRNPA2B1 depletion significantly reduced phosphorylated NF-κB (p-NF-κB) protein levels (**Figure 6A**), while functional assays revealed substantial impairment of malignant phenotypes. MTS proliferation assays showed time-dependent attenuation of cell viability in *HNRNPA2B1*-deficient cells compared to controls (**Figure 6B**). Furthermore, transwell migration and invasion assays exhibited markedly reduced migratory and invasive capacities in *HNRNPA2B1*-depleted cells (**Figure 6C**, **6D**), collectively indicating that *HNRNPA2B1* knockdown attenuates the proliferative and metastatic potential of glioma cells.

To delineate the hierarchical relationship between DERL3 and HNRNPA2B1 in glioma progression, we performed rescue experiments by overexpressing DERL3 in both *HNRNPA2B1*-knockdown and control cells. While *DERL3* overexpression significantly enhanced proliferative, migratory and invasive capacities in control cells (Figure S5A-F), these oncogenic effects were completely abrogated in *HNRNPA2B1*-deficient backgrounds. These results demonstrate that HNRNPA2B1 serves as an essential downstream effector mediating DERL3-dependent activation of NF-κB signaling and subsequent promotion of glioma malignancy.

DERL3 knockdown suppresses GBM progression in an intracranial xenograft model

To validate the tumorigenic role of DERL3 in vivo, we established an orthotopic xenograft model by intracranially implanting U87 glioma cells into nude mice. Histopathological examination (H&E staining) of brain sections harvested 31 days post-implantation revealed significantly reduced tumor volumes in *DERL3*-knockdown groups compared to controls (Figure S6A, S6B). Importantly, Kaplan-Meier survival analysis demonstrated markedly prolonged survival in mice bearing *DERL3*-deficient tumors (**Figure 6E**). Immunohistochemical analysis confirmed successful DERL3 knockdown (**Figure 6F**) and revealed concomitant reduction in Ki67 proliferation index (**Figure 6F**), indicating decreased tumor cell proliferation. These in vivo findings collectively demonstrate that

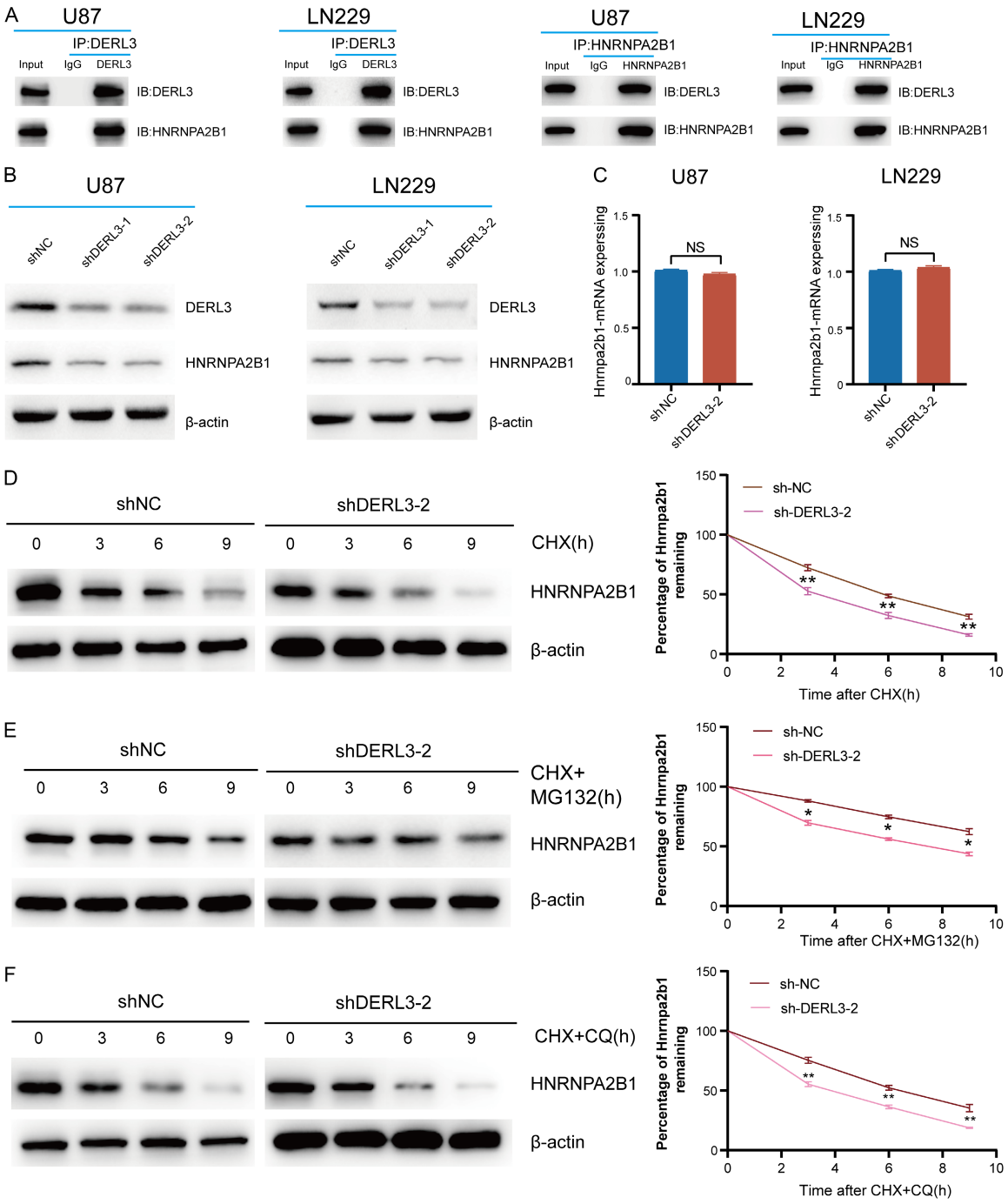

Figure 5. DERL3 maintains its stability by binding to HNRNPA2B1. A. The CO-IP experiment confirmed the binding relationship between DERL3 and HNRNPA2B1 in LN229 and U87 cell lines (HNRNPA2B1 antibody, PTG: 14813-1-AP). B. Western detection showed that DERL3 can regulate HNRNPA2B1 in U87 and LN229 cell lines. C. Knocking down DERL3 did not significantly alter the mRNA expression of HNRNPA2B1 (n=3, unpaired t-test). D-F. The degradation rate and degradation curve of HNRNPA2B1 protein in the DERL3 knockdown group and control group were plotted after the addition of CHX, CHX+MG132, and CHX+CQ (n=3, unpaired t-test).

DERL3 depletion effectively attenuates glioblastoma growth and improves host survival, further supporting its critical role in glioma progression.

Discussion

Gliomas, particularly GBMs, represent the most aggressive and lethal primary brain tumors,

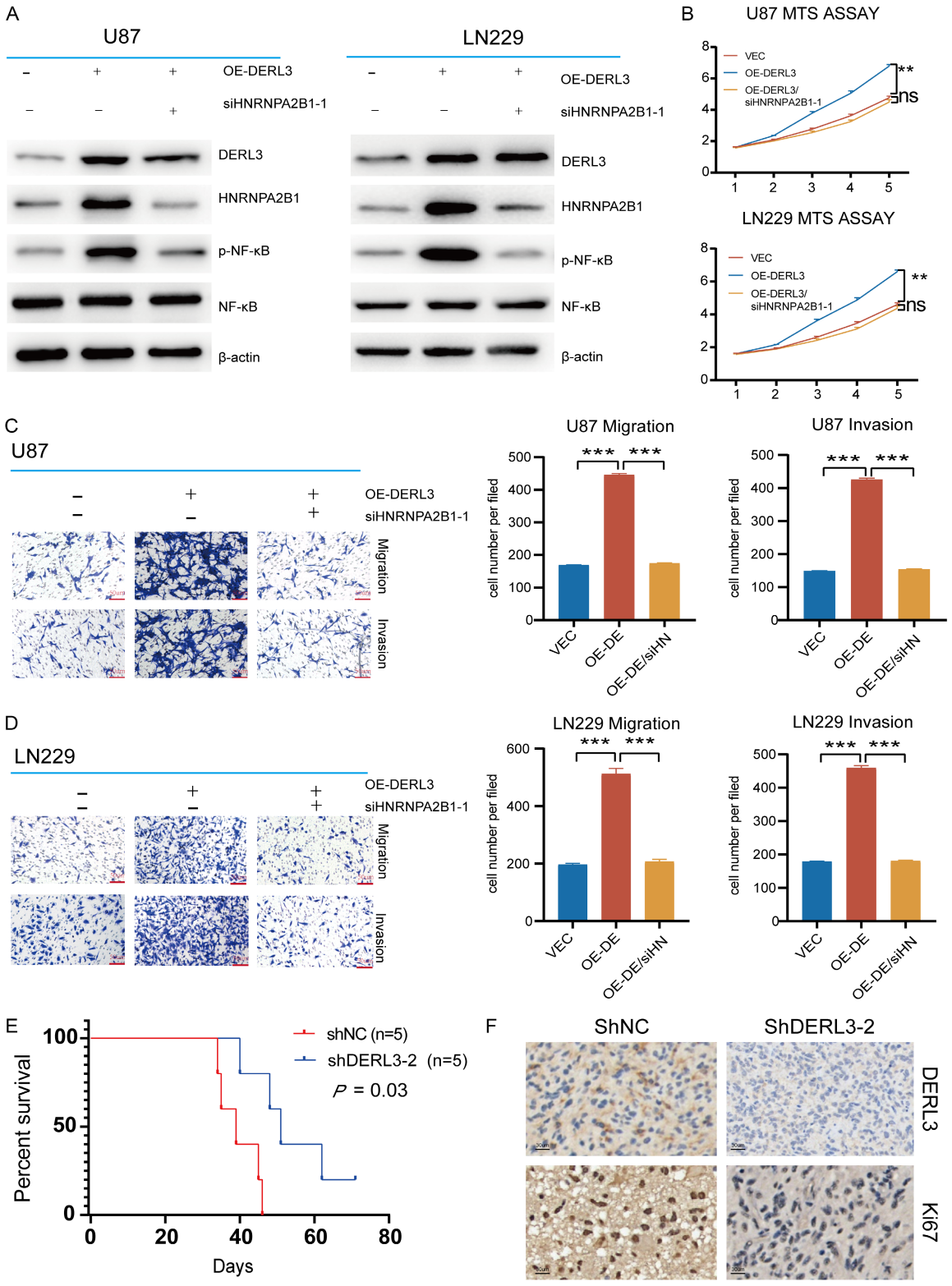

Figure 6. Knockdown of HNRNPA2B1 and DERL3 inhibits malignant progression of GBM. A. In U87 and LN299 cell line, HNRNPA2B1 can regulate the NF-κB signaling pathway. B. Changes in cell migration and invasion after knocking down HNRNPA2B1 in U87 and LN229 cell lines (n=3, two-way repeated-measures ANOVA). C, D. Cell proliferation before and after knocking down HNRNPA2B1 in U87 and LN229 cell lines (n=3, one-way ANOVA; Magnification: 10X). E. The survival of mice in DERL3 knockdown group was significantly prolonged (survival analysis, n=80; log-rank). F. IHC staining of DERL3 and Ki67 in DERL3 control group and knockdown group (Magnification: 40X).

characterized by high mortality rates, significant disability, and substantial economic burdens on healthcare systems globally [17]. The intrinsic plasticity of glioma cells enables rapid adaptation to microenvironmental stressors, contributing to therapeutic resistance and disease recurrence [18]. Recent advances have highlighted the pivotal role of ER stress in tumorigenesis, where it modulates autophagy, oxidative stress, and inflammatory responses via the UPR pathway [19, 20]. While ER stress has been implicated in various malignancies, its specific contributions to GBM pathogenesis remain underexplored. This study aims to characterize ER stress-related molecular signatures in GBMs and evaluate their clinical and therapeutic relevance, with a focus on the derlin family protein DERL3 as a potential prognostic marker and therapeutic target.

Accumulating evidence underscores the involvement of ER stress in cancer progression, where it orchestrates adaptive mechanisms that promote tumor survival and aggressiveness [21]. In gliomas, ER stress activation has been linked to poor prognosis, yet its detailed molecular landscape and clinical implications are poorly defined. To address this gap, we curated a comprehensive gene set associated with ER stress and computed individualized ER stress risk scores for glioma patients. Our analysis revealed a progressive increase in ER stress risk scores with ascending glioma grade, correlating with significantly shorter overall survival in high-risk cohorts. Further stratification demonstrated that patients with elevated ER stress scores frequently harbored IDH1 wild-type status and stromal molecular subtypes, both of which are hallmarks of aggressive glioma biology. These findings suggest that ER stress activation may drive malignant phenotypes in gliomas, particularly in tumors with complex metabolic and microenvironmental dysregulation. The association between ER stress and adverse molecular features underscores its potential as a prognostic biomarker and therapeutic vulnerability in glioma.

To identify key ER stress-related regulators, we performed univariate and multivariate Cox regression analyses on glioma clinical datasets, pinpointing DERL3 as a gene of independent prognostic significance. Located at chromosome 22q11.23, DERL3 encodes a 235-amino acid protein that oligomerizes with other derlin family members (e.g., DERL1/2) and localizes to the ER membrane. As a component of the ER-associated degradation (ERAD) machinery, DERL3 facilitates the clearance of misfolded glycoproteins, thereby maintaining ER homeostasis under stress conditions [22, 23]. Prior studies implicate DERL3 in cancer progression: its knockdown suppresses proliferation and metastasis in lung adenocarcinoma [15], while its overexpression enhances invasiveness in breast cancer [16]. However, its role in glioma remained unexplored. Here, we demonstrate that DERL3 expression escalates with glioma grade, peaking in GBMs, and is predictive of poor patient outcomes. Immunohistochemical and molecular analyses confirmed DERL3 overexpression in high-grade gliomas, positioning it as a robust biomarker for tumor aggressiveness. These results establish DERL3 as a critical mediator of ER stress responses in glioma pathogenesis.

The oncogenic functions of DERL3 were experimentally validated using loss- and gain-of-function models. Silencing DERL3 in GBM cell lines attenuated proliferation, migration, and invasion, whereas its overexpression exacerbated these malignant traits. In vivo, intracranial xenografts with DERL3 knockdown exhibited slower tumor growth and prolonged survival in murine models, reinforcing its pro-tumorigenic role. Mechanistically, DERL3's effects were linked to its interaction with HNRNPA2B1, a RNA-binding protein implicated in mRNA stability and splicing. We found that DERL3 stabilizes HNRNPA2B1, thereby activating the NF-κB signaling pathway - a known driver of glioma progression. This axis underscores DERL3's capacity to integrate ER stress with transcriptional programs that fuel tumor aggressiveness. Our work is the first to delineate the DERL3-HNRNPA2B1-NF-κB pathway in gliomas, offering a novel mechanistic framework for ER stress-mediated adaptation.

The plasticity of GBM cells under stress necessitates innovative therapeutic strategies that disrupt adaptive survival mechanisms. Our identification of the DERL3-HNRNPA2B1-NF-κB axis provides a actionable target for intervention. Precedents in other cancers support this approach: ER stress inhibitors and NF-κB antagonists have shown efficacy in preclinical models. Given DERL3's overexpression in GBMs, small-molecule inhibitors or RNA-based

therapeutics targeting DERL3 could mitigate its oncogenic effects. Furthermore, combining DERL3 inhibition with standard therapies may circumvent resistance rooted in ER stress adaptation. Future studies should prioritize high-throughput screening for DERL3-specific compounds and evaluate their efficacy in orthotopic glioma models. The translational potential of this axis is underscored by the clinical availability of NF-κB inhibitors, which could be repurposed for GBM therapy.

Our further research will focus on the impact of ER stress inducers on DERL3 expression. Tunicamycin, a nucleoside antibiotic that inhibits N-linked glycosylation, disrupts protein folding and thereby induces endoplasmic reticulum (ER) stress, activating the three major unfolded protein response (UPR) pathways: IRE1, PERK, and ATF6. Under such stress, the IRE1 pathway mediates the unconventional splicing of XBP1 mRNA into its active form (XBP1s), which in turn upregulates the transcription of ER-associated degradation (ERAD) genes such as DERL3. This enhances the clearance of misfolded proteins and promotes restoration of ER homeostasis [24-28]. Thapsigargin, an inhibitor of the ER calcium pump SERCA, depletes ER calcium stores and disrupts calcium homeostasis, triggering a global UPR. This comprehensive activation involves coordinated actions of the IRE1, PERK, and ATF6 pathways. Specifically, PERK phosphorylates eIF2α to attenuate global protein synthesis, thereby reducing the protein-folding burden and improving cellular adaptability to folding stress. Moreover, downstream PERK effectors ATF4 and CHOP may indirectly upregulate DERL3 expression, further enhancing ERAD activity to counteract proteostatic stress [25, 29, 30]. Future studies should focus on elucidating the crosstalk between these UPR branches and their temporal coordination in different stress contexts, which may reveal novel therapeutic strategies for diseases linked to ER dysfunction.

This study establishes ER stress as a hallmark of GBM aggressiveness and nominates DERL3 as a central effector of this pathway. By integrating bioinformatics with functional assays, we delineated the prognostic relevance of DERL3 and its role in sustaining GBM malignancy via HNRNPA2B1-NF-κB signaling. while we validated DERL3's expression and prognostic value using multiple public datasets (TCGA, CGGA) and our own IHC cohort, future validation in larger, multi-institutional patient cohorts or tissue microarrays would further strengthen the clinical applicability of our findings. These findings advance the understanding of ER stress in glioma biology and provide a rationale for targeting the DERL3-HNRNPA2B1-NF-κB axis. Future work will focus on developing DERL3-targeted therapies and testing their efficacy in preclinical models, with the ultimate goal of clinical translation. Unraveling the interplay between ER stress and GBM adaptation will be pivotal for overcoming therapeutic resistance and improving patient outcomes.

Conclusion

In conclusion, this study establishes ER stress as a hallmark of GBM aggressiveness and nominates DERL3 as a central effector of this pathway. By integrating comprehensive bioinformatics analyses with rigorous functional validation, we have delineated the prognostic relevance of DERL3 and uncovered its pivotal role in sustaining GBM malignancy. Our work is the first to elucidate a novel ATF6-DERL3-HNRNPA2B1-NF-κB signaling axis, providing a mechanistic link through which ER stress adaptation is translated into pro-tumorigenic outcomes. These findings not only advance our understanding of ER stress in glioma biology but also provide a compelling rationale for targeting the DERL3-HNRNPA2B1-NF-κB axis as a promising therapeutic strategy. Future efforts will focus on developing DERL3-targeted agents and evaluating their efficacy, alone or in combination with standard therapies, in preclinical models, with the ultimate goal of overcoming therapeutic resistance and improving patient outcomes in this devastating disease.

Acknowledgements

This study was supported by the Shenyang Science and Technology Program (2022-321-33-82 to Ren XL) and the Liaoning Provincial Science and Technology Program (2024-BS-029 to Du SN).

All patients gave written informed consent for research use of their surgical specimens and clinicopathological data, and patient anonymity was preserved.

Disclosure of conflict of interest

None.

Abbreviations

CNS, Central nervous system; ER, Endoplasmic reticulum; GBM, Glioblastoma; CGGA, Chinese Glioma Genome Atlas; TCGA, The Cancer Genome Atlas; LGG, Low grade glioma; IDH1, Isocitrate dehydrogenase (NADP (+)) 1; UPR, Unfolded protein response; IP, Immunoprecipitation; OS, Overall survival; IHC, Immunohistochemistry; CHX, Cycloheximide; CQ, Chloroquine.

Address correspondence to: Xiaolin Ren, Shenyang Red Cross Hospital, No. 389 Zhongshan Road, Shenhe District, Shenyang 110013, Liaoning, China. E-mail: 20231162@cmu.edu.cn

References

[1] Louis DN, Perry A, Wesseling P, Brat DJ, Cree IA, Figarella-Branger D, Hawkins C, Ng HK, Pfister SM, Reifenberger G, Soffietti R, von Deimling A and Ellison DW. The 2021 WHO classification of tumors of the central nervous system: a summary. Neuro Oncol 2021; 23: 1231-1251.

[2] Louis DN, Ohgaki H, Wiestler OD, Cavenee WK, Burger PC, Jouvet A, Scheithauer BW and Kleihues P. The 2007 WHO classification of tumours of the central nervous system. Acta Neuropathol 2007; 114: 97-109.

[3] Chinot OL, Wick W, Mason W, Henriksson R, Saran F, Nishikawa R, Carpentier AF, Hoang-Xuan K, Kavan P, Cernea D, Brandes AA, Hilton M, Abrey L and Cloughesy T. Bevacizumab plus radiotherapy-temozolomide for newly diagnosed glioblastoma. N Engl J Med 2014; 370: 709-722.

[4] Wen PY and Kesari S. Malignant gliomas in adults. N Engl J Med 2008; 359: 492-507.

[5] O'Malley J, Kumar R, Inigo J, Yadava N and Chandra D. Mitochondrial stress response and cancer. Trends Cancer 2020; 6: 688-701.

[6] Amaravadi RK, Kimmelman AC and Debnath J. Targeting autophagy in cancer: recent advances and future directions. Cancer Discov 2019; 9: 1167-1181.

[7] Urra H, Aravena R, González-Johnson L and Hetz C. The UPRising connection between endoplasmic reticulum stress and the tumor microenvironment. Trends Cancer 2024; 10: 1161-1173.

[8] Chen X and Cubillos-Ruiz JR. Endoplasmic reticulum stress signals in the tumour and its microenvironment. Nat Rev Cancer 2021; 21: 71-88.

[9] Urra H, Dufey E, Avril T, Chevet E and Hetz C. Endoplasmic reticulum stress and the hallmarks of cancer. Trends Cancer 2016; 2: 252-262.

[10] Chen X, Iliopoulos D, Zhang Q, Tang Q, Greenblatt MB, Hatziapostolou M, Lim E, Tam WL, Ni M, Chen Y, Mai J, Shen H, Hu DZ, Adoro S, Hu B, Song M, Tan C, Landis MD, Ferrari M, Shin SJ, Brown M, Chang JC, Liu XS and Glimcher LH. XBP1 promotes triple-negative breast cancer by controlling the HIF1α pathway. Nature 2014; 508: 103-107.

[11] Jiang HY, Wek SA, McGrath BC, Scheuner D, Kaufman RJ, Cavener DR and Wek RC. Phosphorylation of the alpha subunit of eukaryotic initiation factor 2 is required for activation of NF-kappaB in response to diverse cellular stresses. Mol Cell Biol 2003; 23: 5651-5663.

[12] Yao X, Tu Y, Xu Y, Guo Y, Yao F and Zhang X. Endoplasmic reticulum stress-induced exosomal miR-27a-3p promotes immune escape in breast cancer via regulating PD-L1 expression in macrophages. J Cell Mol Med 2020; 24: 9560-9573.

[13] Varone E, Decio A, Chernorudskiy A, Minoli L, Brunelli L, Ioli F, Piotti A, Pastorelli R, Fratelli M, Gobbi M, Giavazzi R and Zito E. The ER stress response mediator ERO1 triggers cancer metastasis by favoring the angiogenic switch in hypoxic conditions. Oncogene 2021; 40: 1721-1736.

[14] Kang JI, Kim DH, Sung KW, Shim SM, Cha-Molstad H, Soung NK, Lee KH, Hwang J, Lee HG, Kwon YT and Kim BY. p62-induced cancer-associated fibroblast activation via the Nrf2-ATF6 pathway promotes lung tumorigenesis. Cancers (Basel) 2021; 13: 864.

[15] Zhou D, Wang J, Yang K, Zhang L, Zheng Q, Bai J, Hu Y, Mu Q, Yin C and Li H. Mechanism of DERL3 affecting the proliferation, invasion and metastasis of lung adenocarcinoma A549 cells. Zhongguo Fei Ai Za Zhi 2020; 23: 638-645.

[16] Shibata M, Kanda M, Tanaka H, Umeda S, Miwa T, Shimizu D, Hayashi M, Inaishi T, Miyajima N, Adachi Y, Takano Y, Nakanishi K, Takeuchi D, Noda S, Kodera Y and Kikumori T. Overexpression of Derlin 3 is associated with malignant phenotype of breast cancer cells. Oncol Rep 2017; 38: 1760-1766.

[17] Alexander BM and Cloughesy TF. Adult glioblastoma. J Clin Oncol 2017; 35: 2402-2409.

[18] Jayaram MA and Phillips JJ. Role of the microenvironment in glioma pathogenesis. Annu Rev Pathol 2024; 19: 181-201.

[19] Senft D and Ronai ZA. UPR, autophagy, and mitochondria crosstalk underlies the ER stress response. Trends Biochem Sci 2015; 40: 141-148.

[20] Wiseman RL, Mesgarzadeh JS and Hendershot LM. Reshaping endoplasmic reticulum

quality control through the unfolded protein response. Mol Cell 2022; 82: 1477-1491.
[21] Koumenis C. ER stress, hypoxia tolerance and tumor progression. Curr Mol Med 2006; 6: 55-69.
[22] Greenblatt EJ, Olzmann JA and Kopito RR. Derlin-1 is a rhomboid pseudoprotease required for the dislocation of mutant α-1 antitrypsin from the endoplasmic reticulum. Nat Struct Mol Biol 2011; 18: 1147-1152.
[23] Oda Y, Okada T, Yoshida H, Kaufman RJ, Nagata K and Mori K. Derlin-2 and Derlin-3 are regulated by the mammalian unfolded protein response and are required for ER-associated degradation. J Cell Biol 2006; 172: 383-393.
[24] Lee J, Sun C, Zhou Y, Lee J, Gokalp D, Herrema H, Park SW, Davis RJ and Ozcan U. p38 MAPK-mediated regulation of Xbp1s is crucial for glucose homeostasis. Nat Med 2011; 17: 1251-1260.
[25] Sharma S, Le Guillou D and Chen JY. Cellular stress in the pathogenesis of nonalcoholic steatohepatitis and liver fibrosis. Nat Rev Gastroenterol Hepatol 2023; 20: 662-678.
[26] Zhang W, Shi Y, Oyang L, Cui S, Li S, Li J, Liu L, Li Y, Peng M, Tan S, Xia L, Lin J, Xu X, Wu N, Peng Q, Tang Y, Luo X, Liao Q, Jiang X and Zhou Y. Endoplasmic reticulum stress-a key guardian in cancer. Cell Death Discov 2024; 10: 343.
[27] Al Otaibi A, Al Shaikh Mubarak S, Al Hejji F, Almasaud A, Al Jami H, Iqbal J, Al Qarni A, Harbi NKA and Bakillah A. Thapsigargin and tunicamycin block SARS-CoV-2 entry into host cells via differential modulation of unfolded protein response (UPR), AKT signaling, and apoptosis. Cells 2024; 13: 769.
[28] Kim SY, Hwang JS and Han IO. Tunicamycin inhibits Toll-like receptor-activated inflammation in RAW264.7 cells by suppression of NF-kappaB and c-Jun activity via a mechanism that is independent of ER-stress and N-glycosylation. Eur J Pharmacol 2013; 721: 294-300.
[29] Yan B, Liu S, Li X, Zhong Y, Tong F and Yang S. Preconditioning with endoplasmic reticulum stress alleviated heart ischemia/reperfusion injury via modulating IRE1/ATF6/RACK1/PERK and PGC-1alpha in diabetes mellitus. Biomed Pharmacother 2019; 118: 109407.
[30] Fang Z, Gao W, Jiang Q, Loor JJ, Zhao C, Du X, Zhang M, Song Y, Wang Z, Liu G, Li X and Lei L. Targeting IRE1alpha and PERK in the endoplasmic reticulum stress pathway attenuates fatty acid-induced insulin resistance in bovine hepatocytes. J Dairy Sci 2022; 105: 6895-6908.

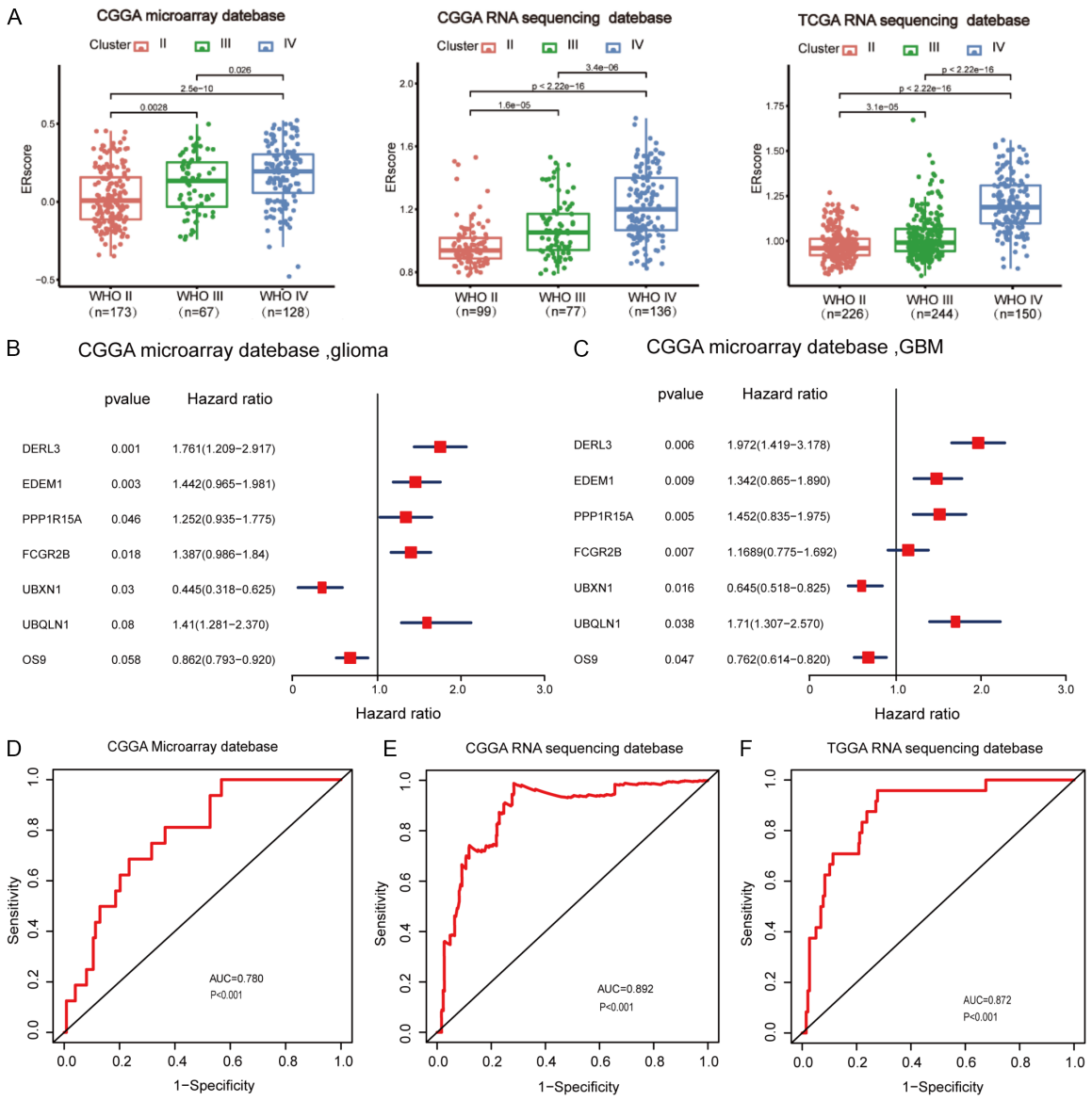

Figure S1. DERL3 as a predictive biomarker for endoplasmic reticulum stress risk in glioma. A. Association between endoplasmic reticulum stress (ERS) risk scores and glioma grade across three independent databases (one-way ANOVA). B. Multivariate Cox analysis of endoplasmic reticulum stress-related genes in CGGA microarray datebase grade gliomas. C. Multivariate Cox analysis of endoplasmic reticulum stress-related genes in CGGA microarray datebase GBM. D. The predictive ability of DERL3 on endoplasmic reticulum risk score in CGGA microarray datebase. E. The predictive ability of DERL3 in CGGA RNA sequencing datebase for endoplasmic reticulum risk score. F. The predictive ability of TCGA RNA database DERL3 for endoplasmic reticulum stress risk score.

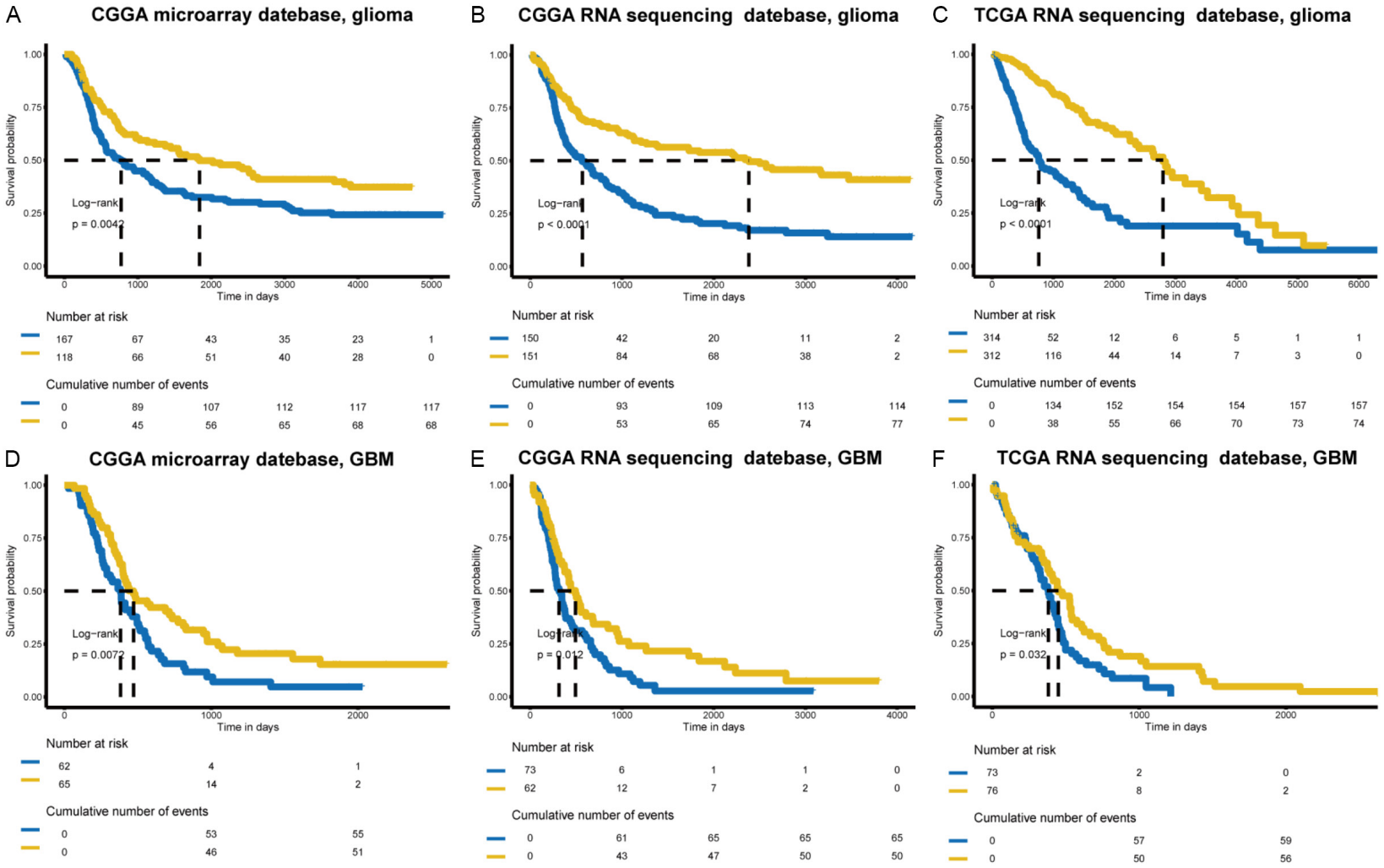
A
CGGA microarray datebase, glioma
Survival probability
Log−rank
p = 0.0042
Time in days
Number at risk
167 67 43 35 23 1
118 66 51 40 28 0
Cumulative number of events
0 89 107 112 117 117
0 45 56 65 68 68
B
CGGA RNA sequencing datebase, glioma
Survival probability
Log−rank
p < 0.0001
Time in days
Number at risk
150 42 20 11 2
151 84 68 38 2
Cumulative number of events
0 93 109 113 114
0 53 65 74 77
C
TCGA RNA sequencing datebase, glioma
Survival probability
Log−rank
p < 0.0001
Time in days
Number at risk
314 52 12 6 5 1 1
312 116 44 14 7 3 0
Cumulative number of events
0 134 152 154 154 157 157
0 38 55 66 70 73 74
D
CGGA microarray datebase, GBM
Survival probability
Log−rank
p = 0.0072
Time in days
Number at risk
62 4 1
65 14 2
Cumulative number of events
0 53 55
0 46 51
E
CGGA RNA sequencing datebase, GBM
Survival probability
Log−rank
p = 0.012
Time in days
Number at risk
73 6 1 1 0
62 12 7 2 0
Cumulative number of events
0 61 65 65 65
0 43 47 50 50
F
TCGA RNA sequencing datebase, GBM
Survival probability
Log−rank
p = 0.032
Time in days
Number at risk
73 2 0
76 8 2
Cumulative number of events
0 57 59
0 50 56

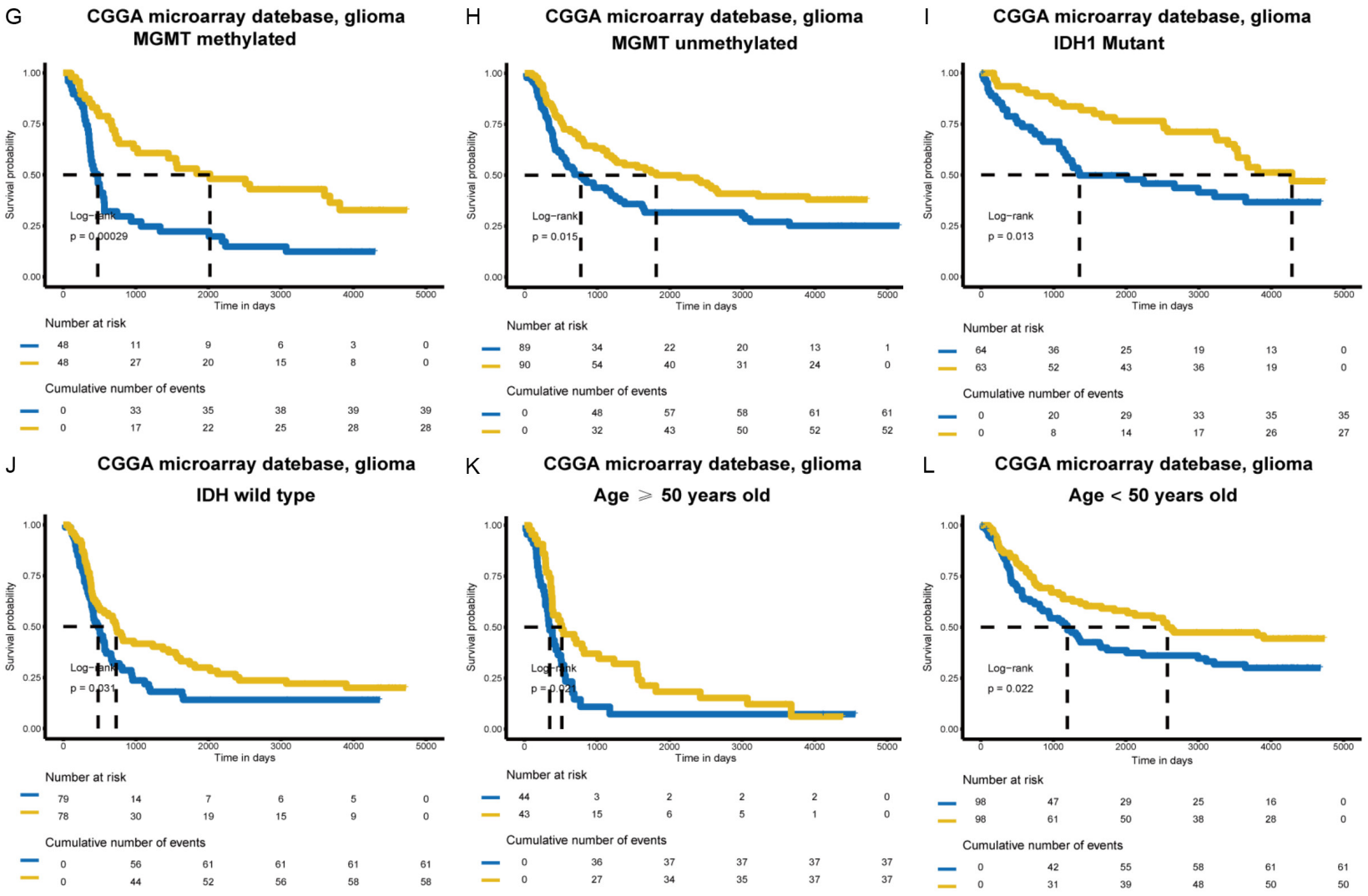

Figure S2. The impact of DERL3 expression on the prognosis of glioma patients. A-C. In CGGA and TCGA databases for all grades of gliomas, the group with high expression of DERL3 had a shorter survival time than the group with low expression. D-F. In CGGA and TCGA databases of GBM, the group with high expression of DERL3 had a shorter survival time than the group with low expression. G, H. Survival curves of high and low endoplasmic reticulum stress risk scores in MGMT promoter state stratified survival analysis in CGGA microarray database. I, J. Survival curves of high and low endoplasmic reticulum stress risk scores in stratified survival analysis based on IDH status in CGGA microarray database. K, L. Survival curves of high and low endoplasmic reticulum stress risk scores in age stratified survival analysis in CGGA microarray database.

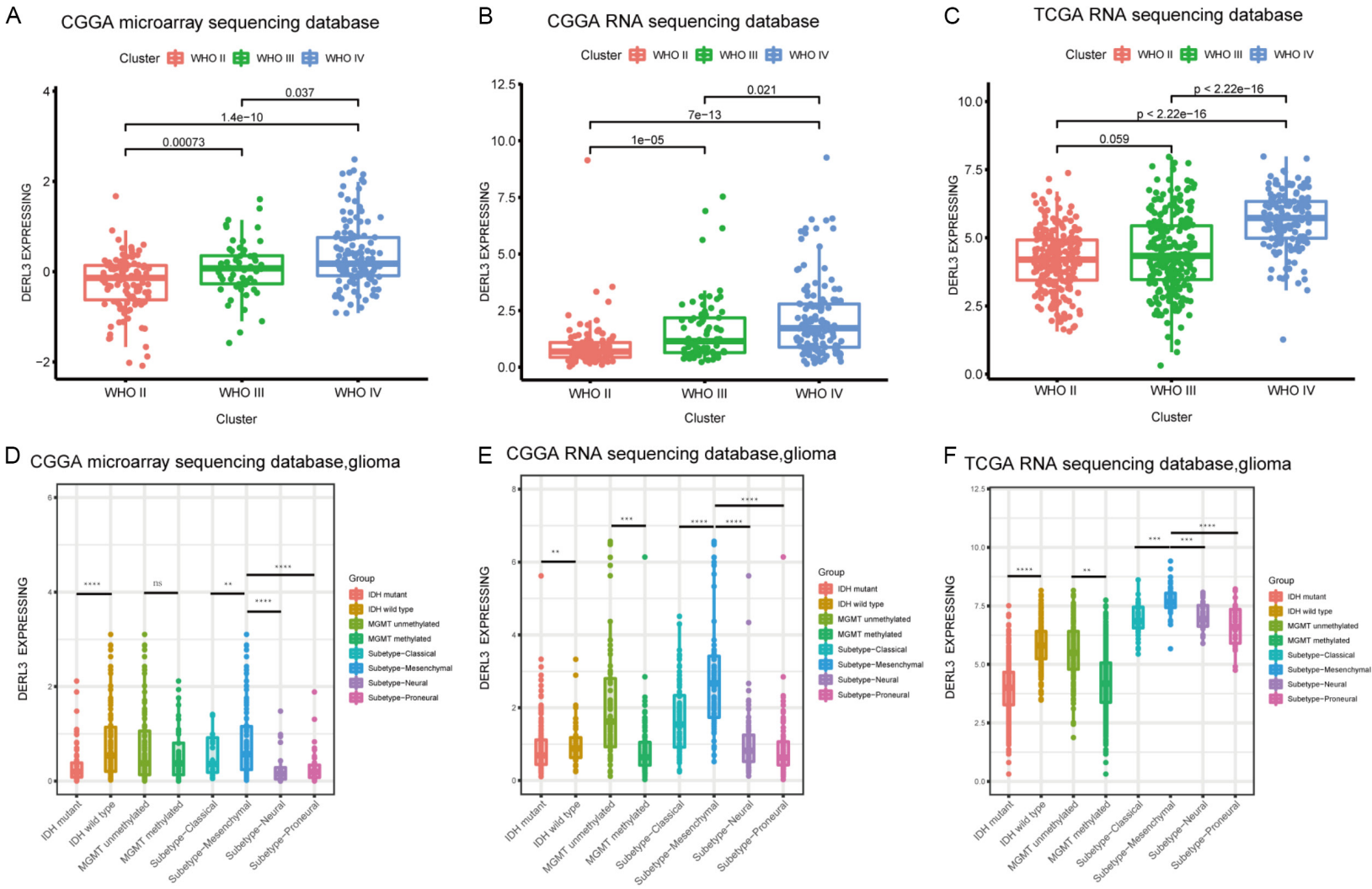
A
CGGA microarray sequencing database
Cluster WHO II WHO III WHO IV
0.037
1.4e−10
0.00073
DERL3 EXPRESSING
WHO II
WHO III
WHO IV
Cluster
B
CGGA RNA sequencing database
Cluster WHO II WHO III WHO IV
0.021
7e−13
1e−05
DERL3 EXPRESSING
WHO II
WHO III
WHO IV
Cluster
C
TCGA RNA sequencing database
Cluster WHO II WHO III WHO IV
p < 2.22e−16
p < 2.22e−16
0.059
DERL3 EXPRESSING
WHO II
WHO III
WHO IV
Cluster
D
CGGA microarray sequencing database,glioma
DERL3 EXPRESSING
Group
IDH mutant
IDH wild type
MGMT unmethylated
MGMT methylated
Subetype−Classical
Subetype−Mesenchymal
Subetype−Neural
Subetype−Proneural
E
CGGA RNA sequencing database,glioma
DERL3 EXPRESSING
Group
IDH mutant
IDH wild type
MGMT unmethylated
MGMT methylated
Subetype−Classical
Subetype−Mesenchymal
Subetype−Neural
Subetype−Proneural
F
TCGA RNA sequencing database,glioma
DERL3 EXPRESSING
Group
IDH mutant
IDH wild type
MGMT unmethylated
MGMT methylated
Subetype−Classical
Subetype−Mesenchymal
Subetype−Neural
Subetype−Proneural

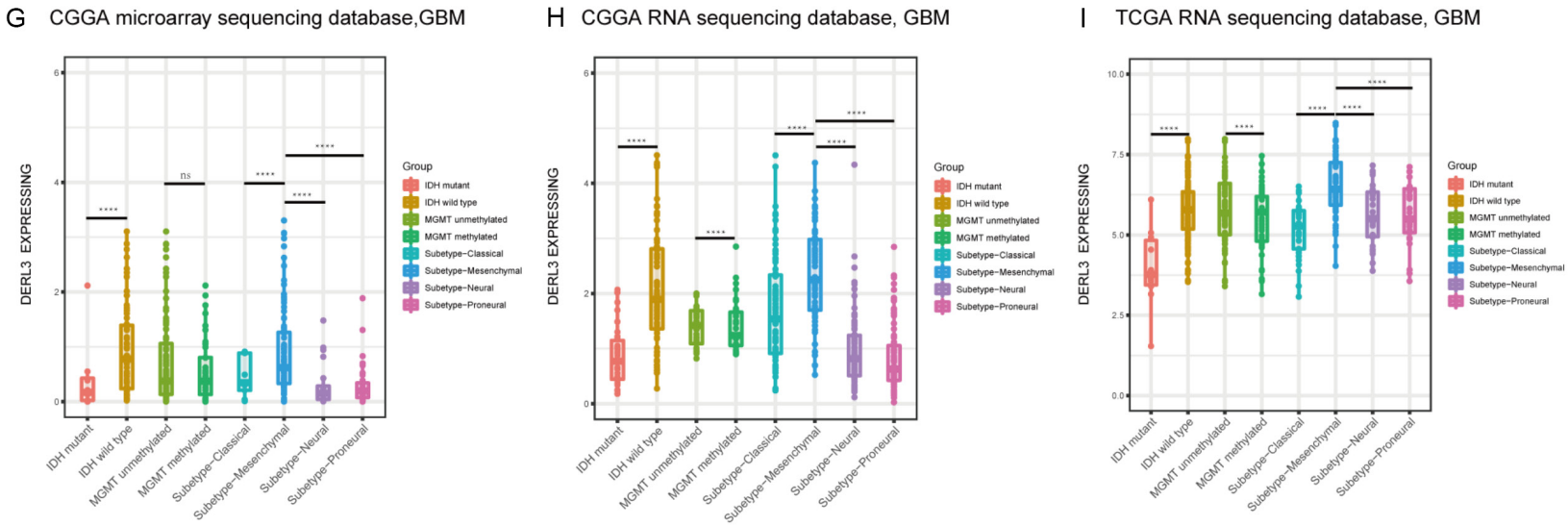

Figure S3. The expression of DERL3 in different subtypes of gliomas. A-C. The expression level of DERL3 changes with the increase of glioma grade in CGGA and TCGA databases (one-way ANOVA). D-I. The expression levels of DERL3 in glioma or GBM different status or subtypes (one-way ANOVA).

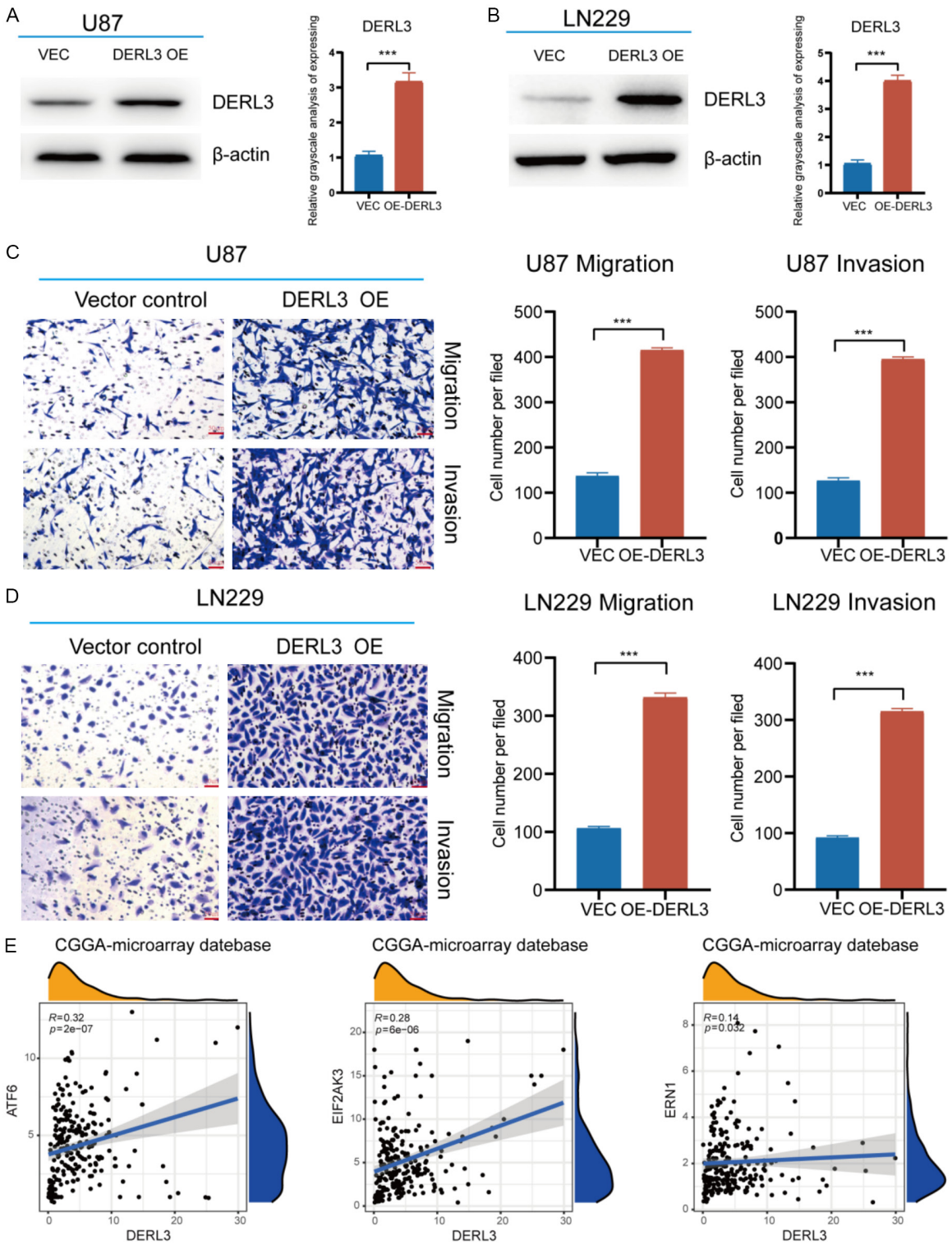

Figure S4. Overexpression of DERL3 effectively promotes malignant behavioral changes in GBM. A, B. Efficiency detection of DERL3 overexpression in U87 and LN229 cells (n=3, unpaired t-test). C, D. Overexpression of DERL3 in U87 and LN229 cells leads to changes in invasion and migration ability (n=3, unpaired t-test; Magnification: 10X). E. The correlation between DERL3 and classical endoplasmic reticulum stress-related pathway markers.

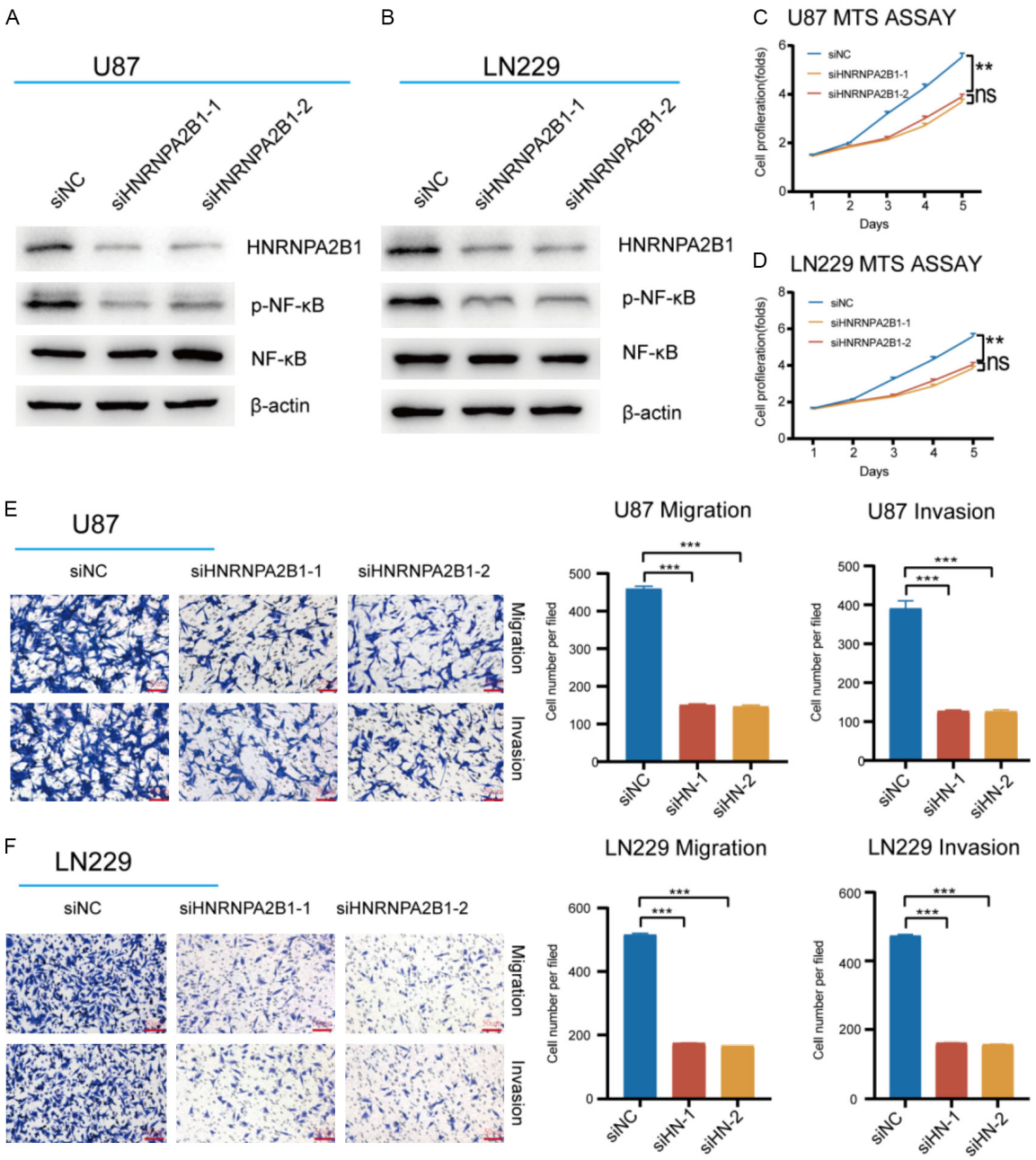

Figure S5. Knocking down HNRNPA2B1 could restore the malignant biological behavior of glioma cells caused by DERL3. A, B. In U87 and LN229 cell lines, DERL3 was overexpressed in siNC and siHNRNPA2B1, respectively, and NF-κB protein expression was detected. C, D. In U87 and LN229 cell lines, after knocking down HNRNPA2B1 and overexpressing DERL3 in the control group, cell proliferation ability was detected (n=3, two-way repeated-measures ANOVA). E, F. In the U87 and LN229 cell lines, after knocking down HNRNPA2B1 and overexpressing DERL3 in the control group, the invasion and migration ability of cells were detected (n=3, one-way ANOVA; Magnification: 10X).

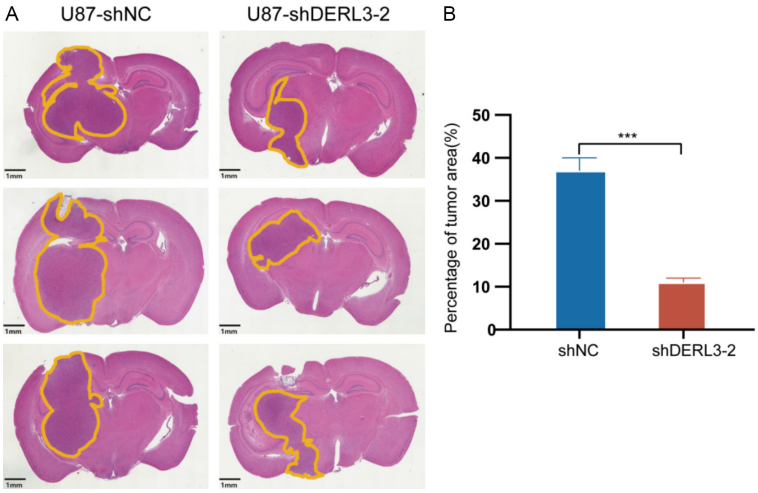

Figure S6. DERL3 silencing decreases intracranial tumor burden in situ. A, B. HE shows that knocking down DERL3 reduces the volume of intracranial tumors in situ (n=3, unpaired t-test; Magnification: 10X).